Assessing the Significance of Dynamic Soil-Structure Interaction by Using Large-Amplitude Mobile Shakers

Sharef Farrag, M.ASCE,¹ Nenad Gucunski, M.ASCE,² Brady Cox, M.ASCE,³ Farnyuh Menq, M.ASCE,⁴ Franklin Moon, M.ASCE,⁵ and John DeVitis, M.ASCE⁶

ABSTRACT

To accurately describe the dynamic characteristics of bridges, it is important in some instances to take into consideration the flexibility and damping of the soil-foundation system. The ability to evaluate those properties in the field can serve as both a check for the design assumptions, and as assistance in the design of bridges with similar superstructure/substructure loading and soil conditions in the future. The goal of the presented study is to demonstrate the use of largeamplitude shaking as an effective tool in measuring actual response/behavior of bridges, and developing better understanding of the dynamic response of bridge systems. For that purpose, a large-amplitude shaking of a bridge in Hamilton Township, New Jersey, was carried out. The T-Rex, a mobile shaker from the Natural Hazards Engineering Research Infrastructure (NHERI) experimental facility at the University of Texas, Austin was employed to shake the bridge. A large number of sensors, geophones and accelerometers, were installed at various locations on the bridge deck, pier cap, and on the adjacent ground to capture the dynamic response of the bridge system. Furthermore, the results from field testing were used to calibrate a 3D finite element model of the bridge. The model was used to conduct a comparative analysis of the bridge response for the assumption of the bridge with fixed foundation conditions, and the bridge with the consideration of dynamic soil-structure interaction (DSSI) effects. The comparison with

¹Department of Civil and Environmental Engineering, Rutgers University, 500 Bartholomew Rd, Piscataway, NJ; e-mail: sharef.farrag@rutgers.edu

²Department of Civil and Environmental Engineering, Rutgers University, 500 Bartholomew Rd, Piscataway, NJ; e-mail: <u>gucunski@soe.rutgers.edu</u>

³Department of Civil and Environmental Engineering, University of Texas, Austin, 1 University Station, Austin, Texas; e-mail: brcox@utexas.edu

⁴Department of Civil and Environmental Engineering, University of Texas, Austin, 1 University Station, Austin, Texas; e-mail: fymenq@utexas.edu

⁵Department of Civil and Environmental Engineering, Rutgers University, 500 Bartholomew Rd, Piscataway, NJ; e-mail: franklin.moon@rutgers.edu

⁶Center for Advanced Infrastructure and Transportation, Rutgers University, 100 Brett Rd, Piscataway, NJ, e-mail: johndevitis@gmail.com

the field testing results demonstrate that the fixed foundation assumption model does not fully capture the behavior of the bridge, as opposed to the model with DSSI considerations.

INTRODUCTION

In the dynamic response analysis of structures, namely bridges, it is commonly assumed that the base of the structure is fixed. However, various research efforts (Antonellis and Panagiotou 2014, Nikolaos et al. 2017) provide more evidence that the effects of the dynamic soil-structure interaction (DSSI) can significantly alter the dynamic response. This is mainly due to the soil-foundation flexibility, and the damping as a result of energy radiation and absorption. The consideration of DSSI in the analysis does not necessarily always entail a detrimental effect on the structure. In most cases it is the opposite. The effect of DSSI on the response will depend on various factors such as the rigidity ratio (ratio of the stiffness of the structure to the same of the soil-foundation system), slenderness ratio (height of the structure to the base width ratio), type of the foundation, and the mass of the structure relative to the mass of the engaged soil-foundation system (Sextos and Manolis 2017).

The evaluation of effects of DSSI on the dynamic response of bridges is largely carried out through numerical simulations (Jian and Nicos 2002, Wang et al. 2014, Sextos et al. 2016). Finite Element Method (FEM) and Boundary Element Methods (BEM) are the primary tools to model the behavior of bridges as a dynamic system. Such large-scale modeling of complex engineering problems is driven by the ever-increasing computational power (Lu et al. 2011). It is noteworthy mentioning that many research efforts utilize either ambient vibrations or historic earthquake records as a source of forced excitation (Bao et al. 2012, Dezi et al. 2012). On the other hand, other research efforts include evaluation of DSSI on scaled models or individual bridge elements, such as piers, in a controlled environment/laboratory (Deng et al. 2012, Manos et al. 2015). Those can be beneficial to evaluate various limit states of bridges. Large amplitude shaking of actual bridges can provide valuable insight about the effects of soil-foundation conditions and design of existing bridges on their dynamic response in a holistic manner.

In the current study, the effects of DSSI on the dynamic response of an actual bridge are assessed via experimental and numerical evaluations. T-Rex, a large-amplitude mobile shaker is used to shake the bridge. T-Rex can be employed to shake the bridge vertically, transversely, and longitudinally. Multiple geophones and accelerometers were placed at various locations on the bridge to capture its dynamic response. Furthermore, numerical simulations were carried out, with the soil-foundation system described by impedance functions to incorporate the effects of DSSI on the response. In addition, a parametric study of a 2D solid-element superstructure/substructure system model was conducted in the frequency domain to evaluate the effects of various soil-foundation-structure parameters. In addition, a 3D finite element model of the tested bridge was- developed and analyzed to compare the results to the field testing results. Some of the findings from the transverse shaking of the bridge, and the corresponding 3D FEM model are presented.

EXPERIMENTAL STUDY

The aim of the experimental program was to carry out large-amplitude shaking of a bridge to capture and develop better understanding of the significance of the DSSI effects on its dynamic response. Hobson Avenue Bridge, a bridge over Interstate 195 in Hamilton Township, New Jersey was selected for the study. It is a 67.4 m [221 ft] two-span steel girder jointed bridge with a three-hammerhead pier on a shallow continuous reinforced concrete (RC) footing. Figure 1 provides a side view of the bridge.



Figure 1. Hobson Avenue Bridge, Hamilton Township, New Jersey.

T-Rex, a mobile shaker from the Natural Hazards Engineering Research Infrastructure (NHERI) experimental facility at the University of Texas at Austin was employed to shake the bridge. The T-Rex, shown in Figure 2, can generate large dynamic forces in any of three directions (vertical, horizontal in-line, and horizontal cross-line). To change from one shaking direction to another, the operator simply pushes a button in the driver's cab. The shaking system is housed on an off-road, all-wheel-drive vehicle. The response of the bridge can be monitored in real-time in a control room. The theoretical force outputs of T-Rex in the vertical and both horizontal directions are shown in Figure 2. The maximum force output is about 267 kN in the vertical mode and about 134 kN in each horizontal mode. The maximum force output is limited by the hold-down weight of the T-Rex truck. Shaking at a higher force output can cause the shaker to decouple (jump) from the ground in the vertical mode or to slide on the ground in the horizontal modes. In a lower frequency range, the force output is limited by the stroke of the reaction mass. In a higher frequency range, the force output is limited by the speed of the hydraulic servo valve. The actual force output depends also on the ground condition, which was not the case in this particular testing.

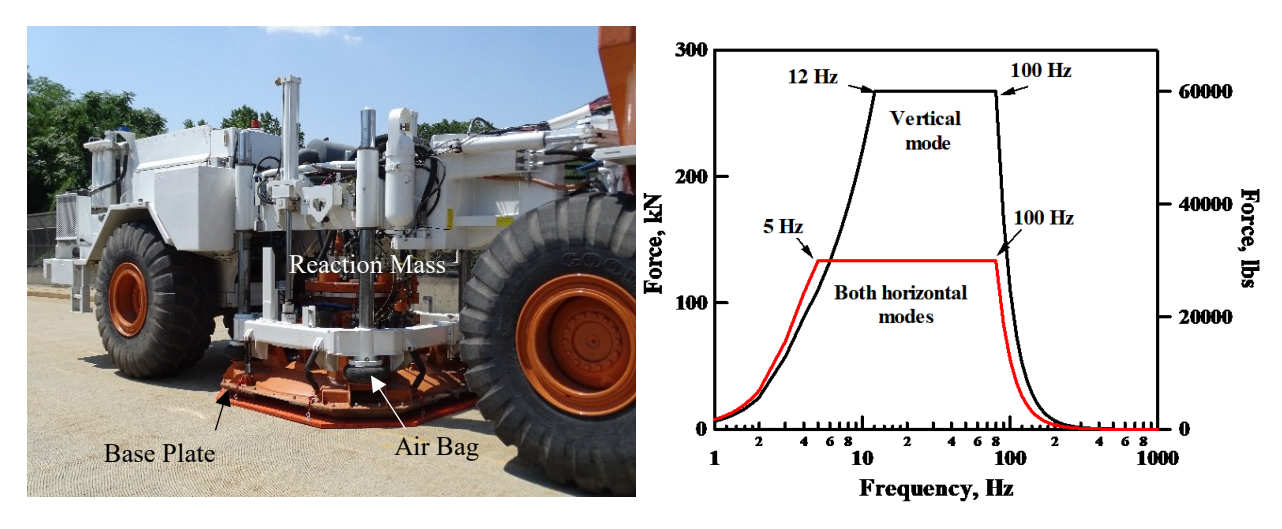


Figure 2. T-Rex (left) and Theoretical force outputs of T-Rex in different modes (right).

To measure the force, T-Rex uses accelerometers mounted on the reaction mass and base plate of the shaker from which the force output can be calculated. As shown in Figure 2, airbags are used to isolate the shaker from the truck. The air bags act as a low pass filter, and transfer only the static force. If a free body of the T-Rex shaker is taken ignoring the hydraulic system, the only external dynamic force is the dynamic ground force, which is also the dynamic force output of T-Rex (Menq et al. 2008, Stokoe et al. 2017).

The T-Rex on-board Pelton controller was modified to provide an external control option. With the external control option, T-Rex can output an arbitrary waveform generated by an analog waveform generator. The amplitude of the force output is proportional to the amplitude of the arbitrary waveform, with the maximum force output set at 5 V of the arbitrary waveform. A Chirp functions was used to drive T-Rex for tests on the bridge. In the chirp function, the frequency of the load varies linearly from the start to end frequency during a given time period. The chirp function is a better option to limit the number of loading cycles, but might always lead to full attainment of a steady state condition. In the current study, a linear chirp was conducted from 15 Hz to 1 Hz, with a total duration of 32 s at a sampling rate of 200 Hz. The driving force was applied at several levels. However, the results presented herein are for the 21 kips [94 kN] force, applied transversely.

Geophone arrays used to capture the deck response and the ground response up to 23 m [80'] away from the bridge due to T-Rex shaking of the bridge are shown in Figure 3. On the other hand, the overall layout of sensors with corresponding channel numbers and locations used to measure the dynamic response of the bridge is shown in Figure 4. A total of 45 geophones were employed in the current study to measure the response at the deck, bent, abutment, and ground.

Prior to the bridge testing, the site's shear wave velocity profile was obtained through Multichannel Analysis of Surface Waves (MASW) testing. The site layout indicating the location of single station horizontal-to-vertical (H/V) spectral ratio noise measurements in the free-field (i.e., well-separated from the structural system), and the 23-m long MASW linear



Figure 3. On the ground geophone arrays (left) and geophone and accelerometer array on the deck (right).

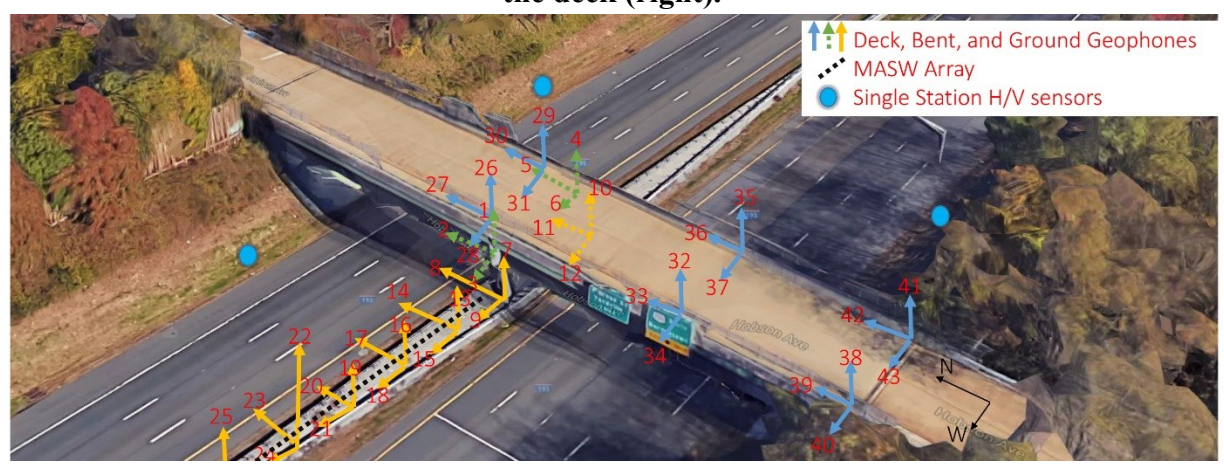


Figure 4. Overall sensors layout.

array, is shown in Figure 4. Each single station measurement location is denoted relative to the Hobson Avenue Bridge (i.e., NW, NE, SW, and SE). To obtain the shear wave velocity (V_s) of the site, various inversion parameterizations for the theoretical fundamental mode Rayleigh wave dispersion considering several layering ratios were evaluated to confirm the experimental data. Figure 5 illustrates the median V_s profiles obtained for the site, showing median V_s profiles derived from the 1000 lowest misfit V_s profiles for each inversion parameterization. The layering ratio (Ξ) representing each inversion parameterization is shown in the figure legend. The layering ratio is followed by the number of layers in the parameterization (inside parentheses) and the H/V curve used to constrain the Rayleigh wave ellipticity peak in the inversion (i.e., SE or SW). The resolution depth (d_{res}), which corresponds to the theoretical resolution limit of the experimental dispersion data (i.e., $d_{res} = \lambda_{max}/2$), is indicated. An average shear wave velocity of 200 m/s is deemed appropriate up to 15 m depth and was used in the numerical modeling.

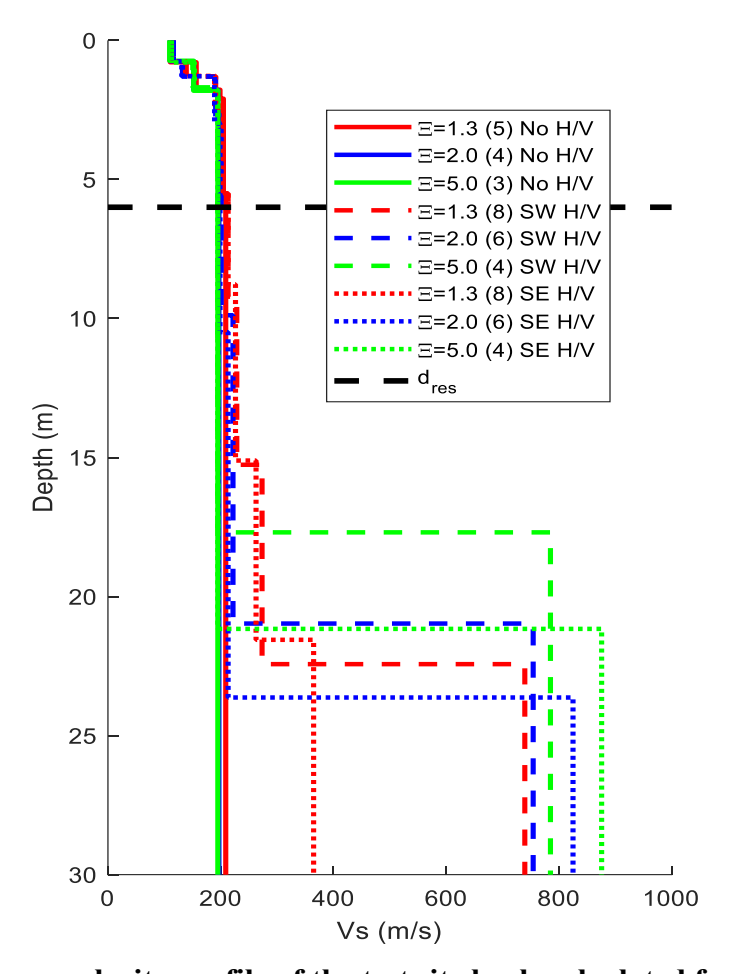


Figure 5. Shear wave velocity profile of the test site back-calculated from the MASW test.

NUMERICAL STUDY

FEM models were developed to capture the effects of DSSI on dynamic response. COMSOL Multiphysics software was used to produce both 2D and 3D FEM simulations of the bridge response due to chirp signal dynamic loading. In both FEM models, linear elastic material properties were selected since the load was in the elastic range. To incorporate the effect of DSSI, the foundation-soil system was modeled as a system of translational and rotational frequency-dependent springs and dashpots, the impedance functions.

Those represent the total mechanical impedance in the $S(\omega) = K(\omega) + i\omega C(\omega)$ form, in which the real part represents the stiffness, while the imaginary part represents the damping. This impedance function can be also written in the form: $K_i = K_{is}[k(\omega) + ia_0c(\omega)]$, where K_i is the total impedance for the i^{th} degree of freedom, K_{is} is the static stiffness of the same degree of freedom, $k(\omega)$ is the stiffness coefficient, $k(\omega)$ is the damping coefficient, $k(\omega)$ is the dimensionless frequency, $k(\omega)$ is the driving frequency, $k(\omega)$ is the half-width (or radius) of the footing, and $k(\omega)$ is the shear wave velocity of the soil. Gazetas (1991) has developed simplified closed-form solutions

for foundations on an elastic half-space, including the effects of foundation shape, embedment, and uniformity of soil. Based on different scenarios, a static stiffness is calculated by knowing the shear modulus of rigidity (G) and geometry of the footing, and then multiplying it by the dynamic coefficients corresponding to the dimensionless frequency of the driving excitation to obtain the dynamic stiffness of the footing. Figure 6 presents an example of the dynamic coefficients used to incorporate the DSSI, demonstrating the change in vertical impedance coefficients as a function of dimensionless frequency. The graphs from Gazetas (1991) were reproduced by the means of cubic splines. This was also carried out for the stiffness and damping of rocking and swaying modes.

For the 2D model, translational and rotational springs were modeled as surface circular footing on an elastic homogeneous half-space as a preliminary approximation of the DSSI. A parametric study was conducted to assess the effect of changing V_s , radius of footing (R), and slenderness ratio (H/W) where H is the height, and W the width of the pier. For the current study, the height was changed and the pier width was held constant. Table 1 illustrates the parameters included in the 2D FEM model of the pier plane section.

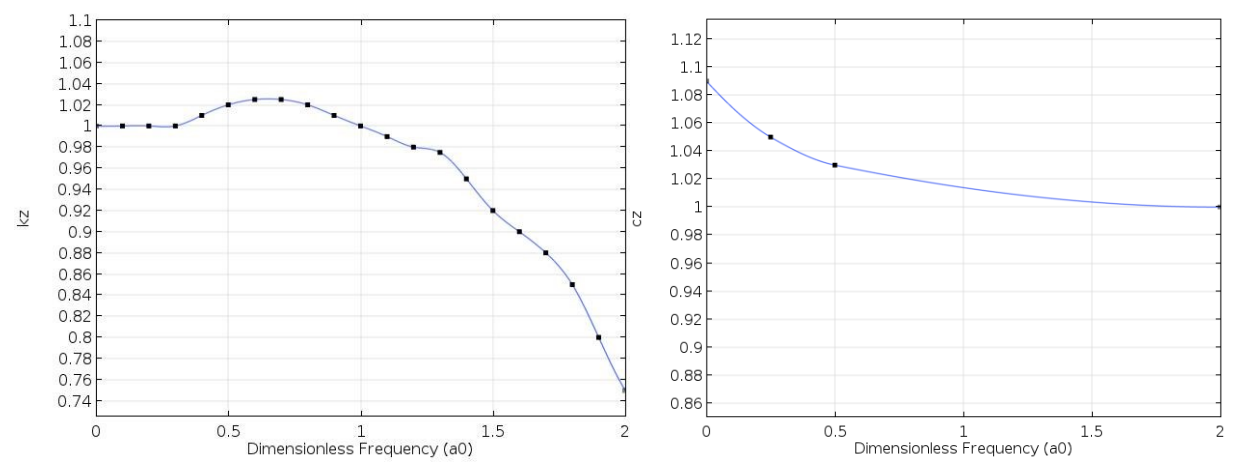


Figure 6. Dynamic vertical spring stiffness (left) and damping (right) coefficients of a surface rectangular footing.

Table 1. Parameters included in the 2D FEM model

Parameter	Description	Expression	Value [unit]	
V _s	Shear Wave Velocity	-	200, 300, 400[m/s]	
R	Footing Radius	-	2, 3, 4 [m]	
H _c	Column Height	-	3-12 @0.5 increments [m]	
μ	Poisson's Ratio of Soil	-	1/3	
$\rho_{\rm s}$	Soil Density	-	1900 [kg/m³]	
G	Modulus of Rigidity	$\rho_{\rm s}({\rm V_s})^2$	Varies: 7.61 x10 ⁷ to 3.04 x10 ⁸ [Pa]	
Ks	Static Sliding Stiffness	$\frac{8GR}{2-\mu}$	Varies: 7.3 x 10 ⁸ to 5.84 x 10 ⁹ [N/m]	
K _r	Static Rocking Stiffness	$\frac{8GR^3}{3(2-\mu)}$	Varies: 9.73 x 10 ⁸ to 3.11 x 10 ¹⁰ [N/rad]	

In addition, a 3D model of the Hobson Avenue Bridge was developed, as shown in Figure 7. A shear wave velocity (200 m/s) determined from the experimental study was used in the description of foundation impedances. The restraint at the ends of the bridge were imposed to reflect simply-supported bridge conditions. Similar to the 2D model, the DSSI was incorporated in the 3D model by a system of translational and rotational springs placed at the bottom of the pier footing defined in Cartesian and spherical coordinates, respectively, utilizing the same approximation of impedance functions as in the 2D model. However, formulae and parameters pertaining to the embedded rectangular foundations in a homogenous half-space were used. The footing vibration modes considered included vertical, transverse and longitudinal swaying, and transverse and longitudinal rocking; torsional vibrations and coupled modes were excluded from the study. Table 2 lists some of the parameters used in the 3D FEM model. A 94 kN [21 k] load was applied transversely.

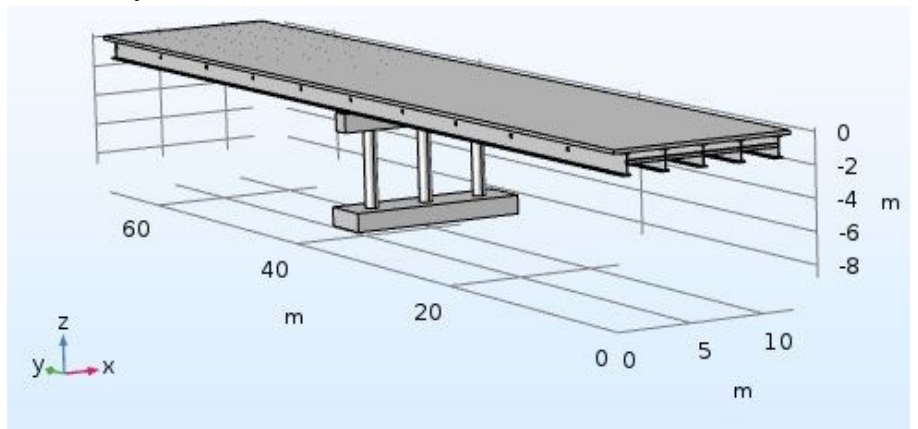


Figure 7. Perspective of the Hobson Avenue bridge model.

Table 2. Parameters included in the 3D FEM model

Parameter	Description	Expression	Value [units]
Kz	Surface Static Vertical Stiffness	$\frac{2GL}{1-\mu}(0.73+1.54\chi^{0.75})$	1.7676 x 10 ⁹ [N/m]
K _y	Surface Static Lateral Stiffness	$\frac{2GL}{2-\mu}(2+2.5\chi^{0.85})$	1.518 x 10 ⁹ [N/m]
K _x	Surface Static Longitudinal Stiffness	$K_{y} - \left[\frac{0.2GL}{0.75 - \mu} \left(1 - \frac{H}{L}\right)\right]$	1.3675 x 10 ⁹ [N/m]
K _{rx}	Surface Static Rocking around x-axis Stiffness	$\frac{GI_{bx}^{0.75}}{1-\mu} \left(\frac{L}{B}\right)^{0.25} \left[2.4 + 0.5 \left(\frac{B}{L}\right)\right]$	8.8458 x 10 ⁸ [N/rad]
K _{ry}	Surface Static Rocking around y-axis Stiffness	$\frac{GI_{bx}^{0.75}}{1-\mu}\left[3\left(\frac{L}{B}\right)^{0.15}\right]$	3.6289 x 10 ⁸ [N/rad]
K _{zemb}	Embedded Static Vertical Stiffness	$K_{z}\left[1+\left(\frac{D_{f}}{21B}\right)\right]\left[1+0.2\left(\frac{A_{w}}{A_{b}}\right)^{2/3}\right]$	2.2104 x 10 ⁹ [N/m]
K _{yemb}	Embedded Static Lateral Stiffness	$K_y \left[1 + 0.15 \left(\frac{D_f}{21B} \right)^{0.5} \right] \left\{ 1 + 0.52 \left[\left(\frac{D_f - H}{B} \right) \left(\frac{A_w}{L^2} \right) \right]^{0.4} \right\}$	1.9262 x 10 ⁹ [N/m]
K _{xemb}	Embedded Static Longitudinal Stiffness	$K_x\left(\frac{K_{yemb}}{K_y}\right)$	1.7353 x 10 ⁹ [N/m]
K _{rxemb}	Embedded Static Rocking around x-axis Stiffness	$K_{rx} \left\{ 1 + 1.26 \left(\frac{D_f - H}{B} \right) \left[1 + \left(\frac{D_f - H}{B} \right) \left(\frac{D_f - H}{D} \right)^{*0.2} \left(\frac{B}{L} \right)^{0.5} \right] \right\}$	2.8324 x 10 ⁹ [N/rad]
K _{ryemb}	Embedded Static Rocking around y-axis Stiffness	$K_{ry}\left\{1 + 0.92\left(\frac{D_f - H}{L}\right)^{0.6} \left[1.5 + \left(\frac{D_f - H}{L}\right)^{1.9}\left(\frac{D_f - H}{L}\right)^{-0.6}\right]\right\}$	1.3986 x 10 ⁹ [N/rad]

RESULTS

2D FEM Pier Section Model: The 2D model was developed to assess certain foundation parameters affecting the structural response of bridges when DSSI is considered. Figure 8 shows the at-resonance peak response at the deck level due to a unit harmonic load applied transversely at the center of the deck. It illustrates that rigidity increases as R.V_s increases, while the response peak amplitude diminishes from 0.0293 m for a flexible foundation (2,200) to 0.014 m as the base becomes infinitely rigid (fixed base), which is expected. An inverse relationship is observed between the resonant frequency and H/W. There is also an effect on curvature of the frequency-H/W graph. Moreover, a fixed-base would experience greater stress level compared to the rocking foundation as illustrated from the response in Figure 9, by which rigidity leads to the restraint of the footing and smaller rotations. Rotation decreased from 0.0032 rad in the flexible foundation (2,200) to around 0.002 rad in the fixed-base model. The effect of changing H/W on rotation is more pronounced than displacement due to the reduced overall rigidity. Therefore, determining the rocking stiffness of the foundation is crucial for predicting the overall response of the system.

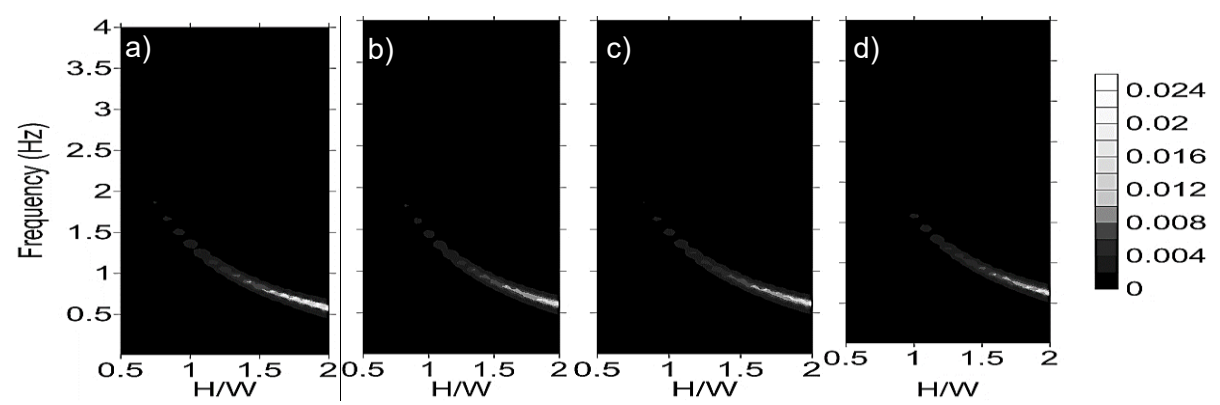


Figure 8. Displacement [m] from 2D FEM model at variable rigidity (R,Vs); a) [2,200], b) [3,300)], c) [4, 400], d) [fixed base].

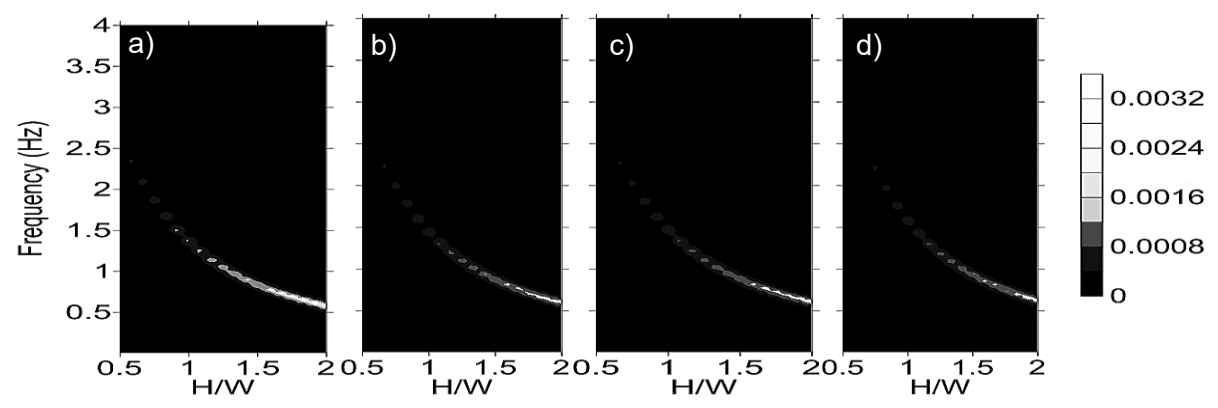


Figure 9. Rotation [rad] from 2D FEM model at variable rigidity (R,Vs); a) [2,200], b) [3,300], c) [4, 400], d) [fixed base].

Field Test: Various bridge response results were obtained from geophones by shaking the bridge, including time histories, response spectra, transfer function, and phase angle at various locations, which are shown in this section.

Figure 10 shows various responses obtained from the test when the bridge was shaken at 94 kN [21 k] transversely. The resonant frequency was 4.61 Hz illustrated in the power spectrum in Figure 10 (b), with a peak response of 0.0512''[0.13 cm] as shown from the time history in Figure 10 (a). Figure 10 (c) and (d) show the vertical response transfer function between channels 28 and 31 (deck west/deck east) and the phase angle respectively. The bridge generally exhibited a similar response on both sides across the sweep, while being out of phase throughout the shaking, which indicates a symmetric response. This describes the rocking of the bridge due to the transverse loading.

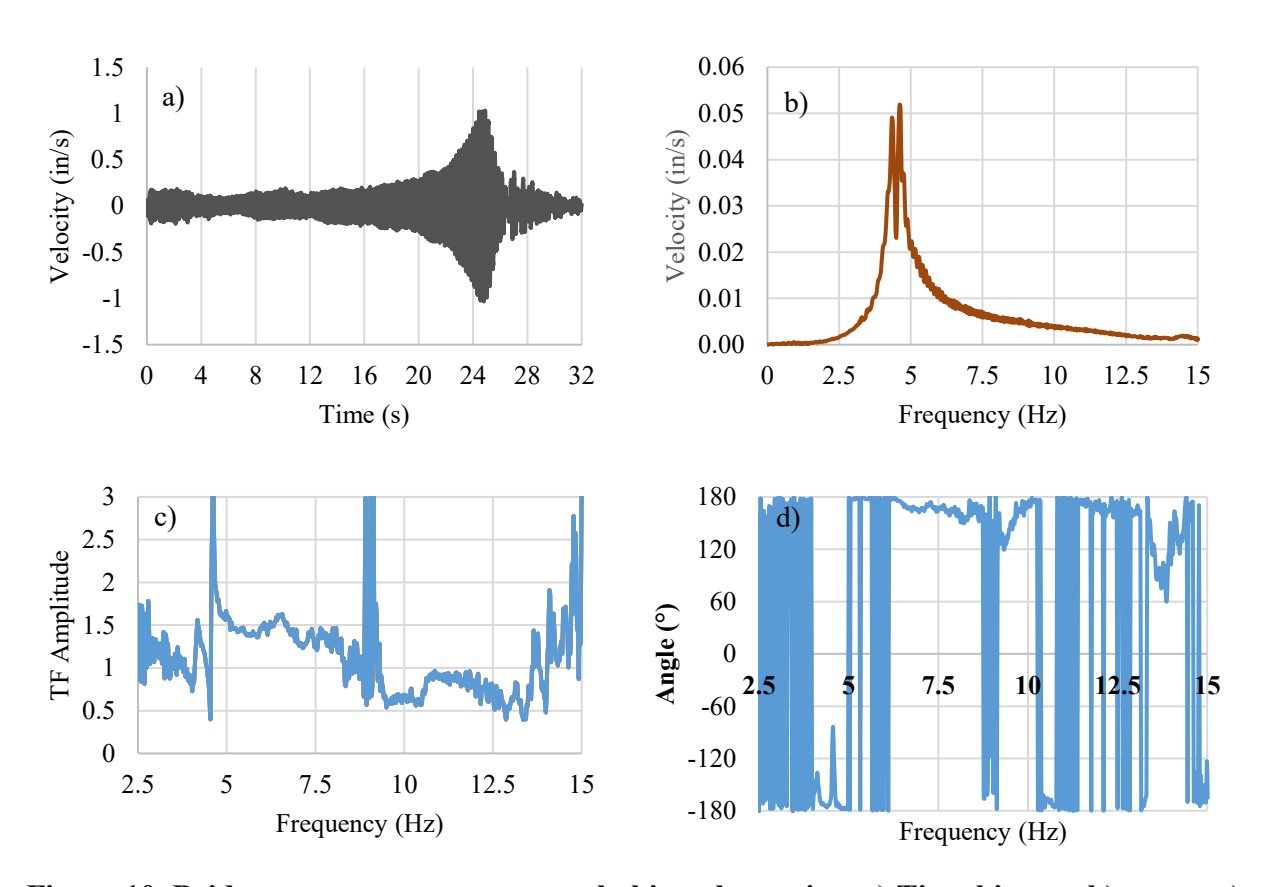


Figure 10. Bridge response to transverse shaking above pier; a) Time history, b) power c) deck east/west transfer function spectrum, d) phase angle.

Comparison of Results with 3D models: A 3D solid-element FEM model of Hobson Ave. Bridge was run developed and used to capture the effect of DSSI on the response. An Eigenmodes study was initially run to identify natural frequencies of dominant modes, as an a priori model. After obtaining the results from the field testing the model was calibrated to closely match the response in a frequency domain study. Once a close match was established, a base fixity was introduced to the model Figure 11 shows a comparison between test, DSSI-

incorporated model, and fixed-base model results. There are two close peaks observed from the test results, occurring at 4.36 and 4.61 Hz, with response amplitudes of 1.23 in/s and 1.3 in/s respectively. The bridge was vibrating in two different modes. In the DSSI-incorporated model, two peaks were also present at 4.20 Hz (3.7% error), and 4.69 Hz (1.74% error). On the other hand, the fixed-base model exhibited one peak at 5.07 Hz (8% error), overshadowing a mode of vibration. The shift in resonant frequency is due to the increased stiffness because of support restraint. A discrepancy was observed on the response of the 1st peak in the DSSI-incorporated model where the response was 1.14 in/s (7.32% error). However, the 2nd peak response (1.29 in/s) was an almost-perfect match with the peak from the test (0.75% error). In both models, the damping at frequencies away from the resonant frequency needs to be further adjusted. Nevertheless, it can be deduced that by assuming a fixed-base, the bridge model will not fully capture the dynamic response as opposed to a case when the DSSI effects are incorporated. Furthermore, numerical simulations of the soil-foundation system are currently carried out to produce more accurate impedance functions, which would ultimately improve the model damping. In addition, a 3D parametric study is to be carried out to assess effects of various super- and substructure parameters on the overall dynamic response of the bridge.

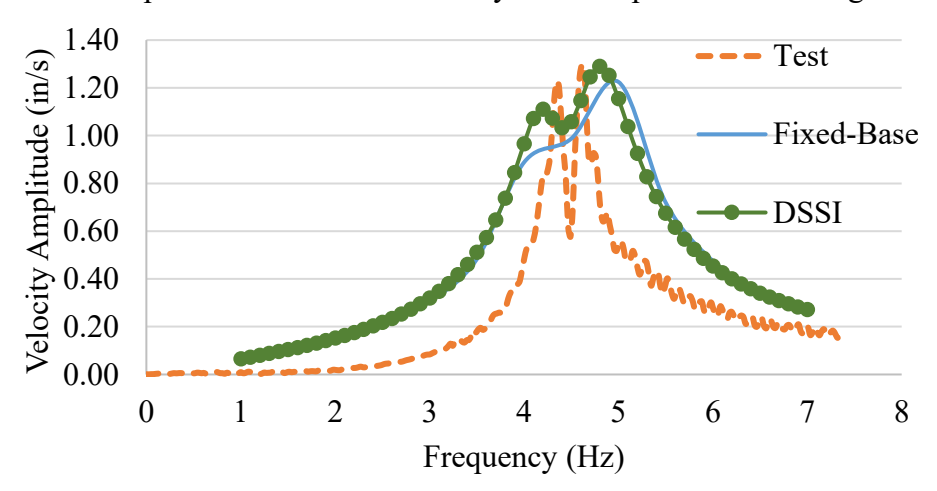


Figure 11. Comparison between response from test, DSSI-incorporated model, and fixed base model.

ACKNOWLEDGMENT

This material is based upon work supported by the National Science Foundation under Grant No. 1650170 and UTA's NHERI@UTexas NSF grant through CMMI-1520808. The support is gratefully acknowledged.

CONCLUSIONS

In the current study, an actual bridge was shaken using a large-amplitude mobile shaker (T-Rex) to capture the effects of DSSI on bridge response. In addition, 2D and 3D models were

established to compare the results with and without incorporating DSSI-effect. Preliminary findings in this paper are:

- Large-amplitude mobile shakers are an effective tool to assess the dynamic response of bridges.
- Increasing the slenderness ratio (H/W) for the same rigidity (R,V_s) leads to a significant increase in response and a reduction in natural frequencies. Increasing the rigidity leads to a reduction of the response amplitude for the same H/W ratio.
- From the experimental frequency sweep, the bridge exhibited two different modes of transverse vibration at 4.36 and 4.61 Hz.
- The DSSI-incorporated model showed an overall better accuracy in terms of capturing the vibrations of the bridge, Eigen-frequencies, and the peak response amplitude than the fixed base model.

REFERENCES

- Antonellis, G. and Panagiotou, M. (2014). "Seismic Response of Bridges with Rocking Foundations Compared to Fixed-Base Bridges at a Near-Fault Site." *Journal of Bridge Engineering*, 19(5).
- Bao, Y., G. Ye, B. Ye and F. Zhang (2012). "Seismic evaluation of soil–foundation—superstructure system considering geometry and material nonlinearities of both soils and structures." *Soils and Foundations*, 52(2): 257-278.
- Deng, L., Kutter, B. L, and Kunnath, S. K. (2012). "Centrifuge Modeling of Bridge Systems Designed for Rocking Foundations." *Journal of Geotechnical and Geoenvironmental Engineering*. 138(3): 335-344.
- Dezi, F., Carbonari, S., Tombari A., and Leoni, G. (2012). "Soil-structure interaction in the seismic response of an isolated three span motorway overcrossing founded on piles." *Soil Dynamics and Earthquake Engineering*, 41: 151-163.
- Gazetas, G. (1991). "Formulas and Charts for Impedances of Surface and Embedded Foundations." *Journal of Geotechnical Engineering*, 117(9): 1363-1381.
- Jian, Z. and Nicos, M. (2002). "Seismic response analysis of highway overcrossings including soil–structure interaction." *Earthquake Engineering & Structural Dynamics*, 31(11).
- Lu, J., Elgamal, A., Yan, L,. Law, K. H., and Conte, J. P. (2011). "Large-Scale Numerical Modeling in Geotechnical Earthquake Engineering." *International Journal of Geomechanics*, 11(6): 490-503.
- Manos, G. C., Pitilakis, K. D., Sextos, A. G., Kourtides, V., Soulis, V., and Thauampteh, J. (2015). "Field Experiments for Monitoring the Dynamic Soil–Structure–Foundation Response of a Bridge-Pier Model Structure at a Test Site." *Journal of Structural Engineering*, 141(1).

- Menq, F.Y., Stokoe, K. H., Park, K. I., Rosenblad, B., and Cox, B. R. (2008). "Performance of Mobile Hydraulic Shakers at NEES@UTexas for Earthquake Studies." 14th World Conference on Earthquake Engineering, Beijing, China.
- Nikolaos, L., Anastasios, S., and Oh-Sung, K. (2017). "Influence of frequency-dependent soil—structure interaction on the fragility of R/C bridges." *Earthquake Engineering & Structural Dynamics*, 46(1): 139-158.
- Sextos, A., P. Faraonis, V. Zabel, F. Wuttke, T. Arndt and P. Panetsos (2016). "Soil–Bridge System Stiffness Identification through Field and Laboratory Measurements." Journal of Bridge Engineering 21(10): 04016062.
- Sextos, Anastasios and Manolis, George (2017). "Dynamic Response of Infrastructure to Environmentally Induced Loads." 1st ed. Vol. 2.
- Stokoe, K., Cox, B., Clayton, P., and Menq, F. (2017). "NHERI@UTexas Experimental Facility: Large-Scale Mobile Shakers for Natural-Hazards Field Studies". *16th World Conference on Earthquake Engineering*, Santiago, Chile.
- Wang, Z., Dueñas-Osorio, L., and Padgett, J. E. (2014). "Influence of Soil-Structure Interaction and Liquefaction on the Isolation Efficiency of a Typical Multispan Continuous Steel Girder Bridge." *Journal of Bridge Engineering*, 19(8).